International Journal of Pharmaceutics 406 (2011) 128–134

Contents lists available at ScienceDirect

International Journal of Pharmaceutics

journal homepage: www.elsevier.com/locate/ijpharm

Pharmaceutical Nanotechnology

Interaction of folate-conjugated human serum albumin (HSA) nanoparticles with tumour cells

Karsten Ulbrich[a], Martin Michaelis[b], Florian Rothweiler[b], Thomas Knobloch[a], Patchima Sithisarn[b], Jindrich Cinatl[b], Jörg Kreuter[a,*]

[a] Institute of Pharmaceutical Technology, Biocenter of Johann Wolfgang Goethe-University, D-60438 Frankfurt am Main, Germany
[b] Institute of Medical Virology, Clinics of the Johann Wolfgang Goethe-University, Paul Ehrlich-Strasse 40, 60596 Frankfurt am Main, Germany

ARTICLE INFO

Article history:
Received 18 August 2010
Received in revised form
14 December 2010
Accepted 17 December 2010
Available online 23 December 2010

Keywords:
Nanoparticles
Human serum albumin (HSA)
Folic acid
Folate receptor
Cancer targeting

ABSTRACT

Folic acid has been previously demonstrated to mediate intracellular nanoparticle uptake. Here, we investigated cellular uptake of folic acid-conjugated human serum albumin nanoparticles (HSA NPs). HSA NPs were prepared by desolvation and stabilised by chemical cross-linking with glutaraldehyde. Folic acid was covalently coupled to amino groups on the surface of HSA NPs by carbodiimide reaction. Preparation resulted in spherical HSA NPs with diameters of 239 ± 26 nm. As shown by size exclusion chromatography, 7.40 ± 0.90 μg folate was bound per mg HSA NPs. Cellular NP binding and uptake were studied in primary normal human foreskin fibroblasts (HFFs), the human neuroblastoma cell line UKF-NB-3, and the rat glioblastoma cell line 101/8 by fluorescence spectrophotometry, flow cytometry, and confocal laser scanning microscopy. Covalent conjugation of folic acid to HSA NPs increased NP uptake into cancer cells but not into HFFs. Free folic acid interfered with cancer cell uptake of folic acid-conjugated HSA NPs but not with uptake of folic acid-conjugated HSA NPs into HFFs. These data suggest that covalent linkage of folic acid can specifically increase cancer cell HSA NP uptake.

1. Introduction

The use of cytotoxic anticancer drugs is limited by high toxicity, rapid elimination from the systemic circulation, accumulation in non-targeted organs and tissues, enzymatic and hydrolytic degradation, and/or inefficient cell entry. In addition, the development of novel anti-cancer drug candidates is often limited by problems including poor solubility in water, unfavourable body distribution, and the inability to cross cellular barriers (Tosi et al., 2008). Large efforts are ongoing to develop drug carrier systems that improve drug performance. In this context, different types of drug carrier systems are under investigation, including nanoparticles (NPs) (Tosi et al., 2008), liposomes (Hattori et al., 2009), dendrimers (Thomas et al., 2010), micelles (Li et al., 2009), carbon nanotubes (Heister et al., 2009), molecular conjugates (Dosio et al., 2009), and quantum dots (Gao et al., 2009). Nano-scaled carriers may mediate improved cell entry, and protect therapeutic agents from degradation in the biological environment. Moreover, nanoparticles may enable the administration of poorly water-soluble drugs. Additionally, surface modifications may allow an enhanced delivery to the desired organs or tissues (Ma, 2008). Also, targeting has been shown to be augmented by the so-called "enhanced permeability and retention (EPR)" effect into malignant tumours (Maeda et al., 2000; Tosi et al., 2008).

NPs can be prepared from different synthetic or natural macromolecular materials. Human serum albumin (HSA) NPs offer several advantages: Since many drugs show a high albumin binding they can be effectively incorporated in the HSA NP matrix. Additionally, the albumin molecules posses certain functional groups that are available on the particle surface for the covalent attachment of drugs or of drug targeting ligands (Langer et al., 2000; Michaelis et al., 2004; Wartlick et al., 2004; Steinhauser et al., 2006; Ulbrich et al., 2009). The introduction of hydrophilic, sterical barriers such as poly(ethylene glycol) chains on the particle surface decreases opsonisation and elimination by the reticuloendothelial system (RES) resulting in long-circulating NPs (Barratt, 2003).

Tumour cells differ in their biology and physiology from normal cells and show (increased) expression of surface markers that may be exploited for drug targeting approaches. Highly proliferating cancer cells need a continuous supply of vitamins and therefore tend to express high levels of vitamin receptors on their cell surfaces (Satyam, 2008). Elevated expression of the folate receptor (FR) was found in various types of human cancers (Leamon, 2008; Parker et al., 2005) or example in 97% of investigated ovarian carcinomas

* Corresponding author at: Institute for Pharmaceutical Technology, Biocenter of Johann Wolfgang Goethe-University, Max-von-Laue-Str. 9, D-60438 Frankfurt am Main, Germany. Tel.: +49 69 798 29682; fax: +49 69 798 29694.
E-mail address: kreuter@em.uni-frankfurt.de (J. Kreuter).

0378-5173/$ – see front matter © 2011 Elsevier B.V. All rights reserved.
doi:10.1016/j.ijpharm.2010.12.023

Table 1
Particle diameter of modified HSA nanoparticles (mean ± S.D.; $n = 10$).

Physicochemical characteristics	Unmodified	Modification with EDC	Covalent binding of folic acid	Adsorptive binding of folic acid
Particle size [nm]	156 ± 25	178 ± 35	239 ± 26	280 ± 92
Polydispersity	0.034 ± 0.022	0.033 ± 0.028	0.030 ± 0.026	0.133 ± 0.126
Zeta potential [mV]	−42 ± 8	−30 ± 13	−37 ± 8	−40 ± 7
Folic acid binding effciency [μg/mg]			7.40 ± 0.90	10.22 ± 2.83
Particle content [mg/ml]	18.3 ± 1.1	19.3 ± 2.0	11.6 ± 2.3	9.5 ± 2.8

(14% weak increase, 39% moderate increase, 44% strong increase). It is weakly (63%) or not at all (37%) expressed in normal tissues including the lung, thyroid, and kidney (Sudimack and Lee, 2000). Moreover, cancer cells typically express α-folate receptors (FRs) while normal cells express β-FRs (Markert et al., 2008). The free R-carboxylic acid that is present on the surface of folate-conjugated drug delivery systems was shown to exhibit a higher affinity for the α-FRs present on cancer cells (Park et al., 2005), while the β-FRs found on normal cells preferentially interact with the reduced form of folic acid, 5-methyltetrahydrofolate (Elnakat and Ratnam, 2004).

Folic acid is also an attractive targeting molecule because of its low immunogenicity, small molecular weight (Mw ~441.4 g/mol), and its compatibility with organic solvents used during the preparation process (Vandervoort and Ludwig, 2002). Additionally, folate-conjugated poly(lactic-co-glycolic acid)-polyethylene glycol (PLGA-PEG), hyperbranched block copolymer-poly(lactic acid) H40-PLA or PLGA-PLA NPs showed pro-longed maintenance in tumours in comparison to nontargeted NPs (Esmaeili et al., 2008; Nie et al., 2009; Prabaharan et al., 2009). After adminstration, the NPs accumulated in tumour cells and liver tissue and remained detectable for four days or even longer than other non-targeted NPs (Kukowska-Latallo et al., 2005). In previous studies transferrin and insulin had successfully been attached to the activated HSA NP with Traut's reagent in order to react with the maleimide crosslinker NHS-PEG-MAL-5000 (Ulbrich et al., 2011). In the present study, folic acid was covalently linked to HSA NPs and NP uptake was studied in human neuroblastoma (UKF-NB-3) and rat glioblastoma (101/8) cells, representing two cell lines that can be targeted by the use of folic acid (Ciofani et al., 2008; Feng et al., 2010). Moreover, both cell lines are models for cancer diseases with a poor outcome. For glioblastomas, the prognosis is very grim with a median survival of 12–15 months (Wen and Kesari, 2008). In the animal model, the rat glioblastoma cell line 101/8 shows diffusely invading growth characteristic resembling the morphology and histology of clinical human glioblastomas (Steiniger et al., 2004; Hekmatara et al., 2009). The second cell line is a neuroblastoma line. Neuroblastomas represent the most frequently occuring solid peripheral tumour of childhood. High-risk disease associated with overall survival rates lower than 40% is diagnosed in about half of patients. MYCN amplification is a strong predictor of poor outcome in neuroblastomas (Maris et al., 2007). The MYCN-amplified neuroblastoma cell line UKF-NB-3 used in this study was isolated from the bone marrow of a patient who died from disease (Kotchetkov et al., 2005).

2. Materials and methods

2.1. Reagents

Batch 016K7546 of human serum albumin (HSA, fraction V, purity 96–99%), glutaraldehyde 8% solution, and N-(3-dimethylaminopropyl)-N-ethylcarbodiimide (EDC) were obtained from Sigma (Steinheim, Germany); 3-(4,5-dimethyl-2-thiazolyl)-2,5-diphenyl-2H-tetrazolium bromide (MTT) was obtained from Serva (Heidelberg, Germany). Folic acid crystalline was from Biochemika (Düsseldorf, Germany). Alexa594-concanavalin A was from Molecular Probes (MoBiTec, Goettingen, Germany), Flouraldehyde™ reagent solution from Pierce (Illinois, USA); PBS, glutamine, penicillin/streptomycin, and trypsin were purchased from Invitrogen GmbH (Karlsruhe, Germany). Sodium dihydrogenphosphate, sodium chloride, disodium hydrogen phosphate, 0.1 N sodium hydroxide, and all other reagents were obtained from Merck Serono (Darmstadt, Germany) and were of analytical grade and used as received.

2.2. Preparation of human serum albumin nanoparticles (HSA NPs)

HSA NPs were prepared by an established desolvation process (Weber et al., 2000; Ulbrich et al., 2009): Two hundred milligram HSA in 2.0 ml 10 mM NaCl solution, adjusted to pH 8.4, were formed into NPs by continuous (1 ml/min) addition of 8.0 ml desolvating agent ethanol under constant stirring at room temperature. After protein desolvation 235 μl of a 8% aqueous glutaraldehyde solution were added to achieve particle crosslinking. The resulting nanoparticles were purified by three cycles of differential centrifugation (16,100 × g, 10 min) and redispersion of the pellet to the original volume in water. The NP content of the suspension was determined by gravimetry.

Table 2
Particle stability of modified HSA nanoparticles (mean ± S.D.; $n = 3$).

	Time [h]			
	0	2	6	24
HSA-NP				
Particle size [nm]	156 ± 25	157 ± 27	175 ± 26	193 ± 22
Polydispersity	0.034 ± 0.022	0.388 ± 0.140	0.512 ± 0.117	0.391 ± 0.224
Folate-adsorbed HSA NP				
Particle size [nm]	250 ± 24	283 ± 36	300 ± 45	316 ± 33
Polydispersity	0.051 ± 0.027	0.178 ± 0.100	0.276 ± 0.160	0.394 ± 0.250
Covalently folate-conjugated HSA NP				
Particle size [nm]	235 ± 24	241 ± 27	254 ± 20	276 ± 29
Polydispersity	0.035 ± 0.031	0.343 ± 0.138	0.410 ± 0.170	0.389 ± 0.104

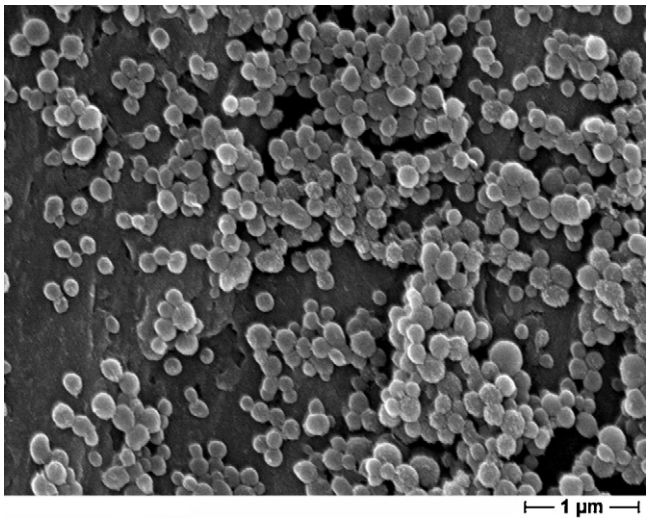

Fig. 1. Scanning electron micrograph (SEM) of human serum albumin nanoparticles prepared in the presence of ethanol after centrifugation and redispersion in water. Bar: 1000 nm.

2.3. Preparation of folate-conjugated human serum albumin nanoparticles (HSA NPs)

HSA NPs, prepared as described above, were modified as follows: 800 μL of folic acid solution (20 mg/ml) in 0.1 N sodium hydroxide were incubated with 200 μL fresh N-(3-dimethylaminopropyl)-N-ethylcarbodiimide (EDC) under constant shaking in the dark for 15 min at 20 °C (Eppendorf thermomixer, 1400 rpm). Subsequently, one millilitre of HSA nanoparticle suspension (content 15 mg/ml) was added, and shaking continued for 1 h. Reaction was stopped by adding 100 μL hydroxylamine (500 mg/ml). The folate-conjugated nanoparticles were then purified from unreacted folic acid by three cycles of differential centrifugation (16,100 × *g*, 10 min) and redispersion of the pellet to the original volume in water.

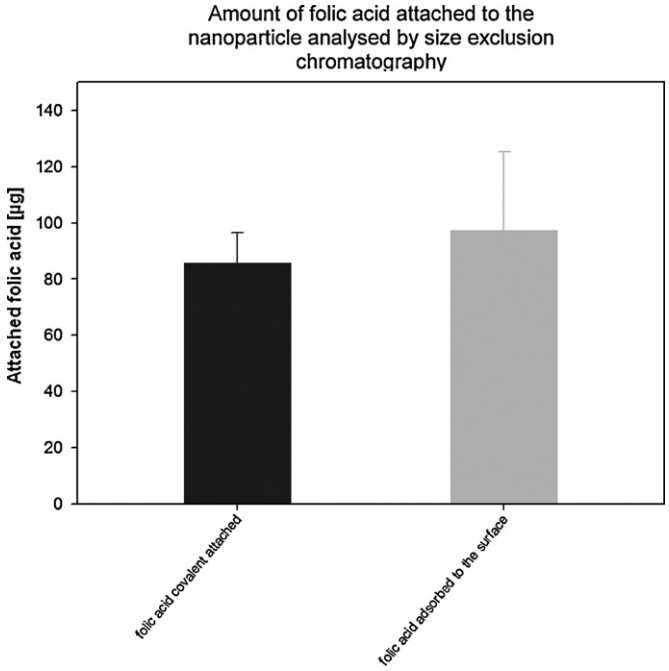

Fig. 2. Amount of attached folic acid to human serum albumin nanoparticles [μg/mg NP] analysed by size exclusion chromatography (SEC) (mean ± S.D.; $n = 3$).

2.4. Characterisation of nanoparticles (NPs)

2.4.1. Size exclusion chromatography (SEC)

After centrifugation of the folate-conjugated HSA NPs, the supernatants containing unbound folic acid were analysed at 280 nm by (absorbance detector: Waters 468) using a Bio SEP SEC 3000 (Phenomenex, Aschaffenburg) column and a pre-column (8 mm × 50 mm) (Bae et al., 2005). The retention times were 7 min for human serum albumin and 12 min for the monomer of folic acid. The HPLC pump (Waters 600) was operated at 1 ml/min using phosphate buffer pH 6.6 as the mobile phase. The supernatants were added to the mobile phase 1:1, samples of 20 μL were injected with an autosampler (Thermo Seperation Products AS100). The unbound fraction of folate was subtracted from the total folate in order to calculate the amount of folic acid coupled to the HSA NPs.

2.4.2. Determination of the particle size and zeta potential

Particle size, polydispersity, and the zeta potential of the NPs were measured by a Malvern Zetasizer 3000 HSA (Malvern, Instruments Ltd., Malvern, UK) at 25 °C and a scattering angle of 90° after an at least 200-fold dilution with purified water. For the zeta potential measurement, the Zetasizer was equipped with a dip-cell (Malvern Instruments Ltd., Malvern, UK).

2.4.3. Determination of particle content and measurement of the particle density

The particle content was determined by gravimetry. 50 μL of the NP suspension was pipetted into an aluminium weighing dish and dried for 2 h at 80 °C. After 30 min of storage in a desiccator, the samples were weighed on a microbalance (Sartoruis, Germany). The particle density was calculated based on the density of the aqueous nanoparticle suspension in comparison to the density of the dispersion medium water using a DMA 48 density meter (AP Paar, Graz, Austria). Calculations were based on the following equation:

$$\rho_p = \frac{\rho_s c}{\rho_L + c - \rho_s}$$

where ρ_p is the nanoparticle density (g cm^{-3}), ρ_s the density of the aqueous nanoparticle suspension (g cm^{-3}), ρ_L the density of the dispersion medium (water) (g cm^{-3}), and c the nanoparticle concentration in the suspension (g cm^{-3}).

2.4.4. Particle stability in cell culture medium

For the determination of the particle stability in cell culture medium, the NPs were incubated at concentrations of 0.1, 0.2, 0.5, and 1.0 mg/ml and 80 μg/ml folic acid for 1, 4, 6, 24, and 48 h at 37 °C in the cell culture medium under shaking. The following preparations were employed: HSA NP without folic acid, HSA NP with covalently bound folic acid, and HSA NP with adsorbed folic acid. The influence of the medium on the particle stability was analysed by size measurements as described above.

2.4.5. Quantification of amino groups on the HSA NP surfaces

The determination of amino groups was performed using Flouraldehyde™ amino assay reagent solution and a fluorescence microplate reader (FLOURstar, excitation wavelength 360 nm, emission wavelength 455 nm). An aliquot (50.0 μL) of the reagent solution was added to 200 μL nanoparticles in a 96-well plate (Greiner bio-one, Frickenhausen, Germany), and the fluorescence was read after 5 min. The content of amino groups was determined by measuring the amount of free amino groups on the particle surfaces with Flouraldehyde™ using 1,4-diaminobutane for the preparation of a calibration curve.

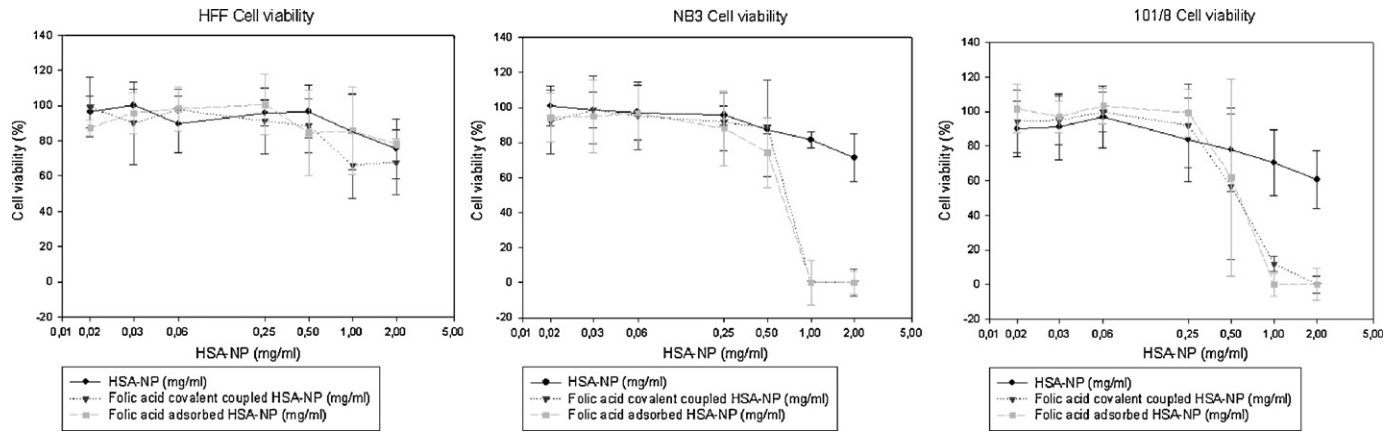

Fig. 3. Cell viability of unmodified and modified HSA NPs treated cells. The cells were incubated with different concentrations of nanoparticles: 0.01 mg/ml, 0.02 mg/ml, 0.06 mg/ml, 0.25 mg/ml, 0.5 mg/ml, 1.0 mg/ml and 2.0 mg/ml for 144 h incubation time (mean ± S.D.; $n = 9$).

2.5. Cells

The human neuroblastoma cell line UKF-NB-3 was isolated and established as described before (Kotchetkov et al., 2005). The cell line 101/8 was isolated from a rat glioblastoma. Human foreskin fibroblasts (HFFs) were isolated as described before (Cinatl et al., 1994). All cell lines were propagated in IMDM supplemented with 10% FCS, 100 IU/ml penicillin, and 100 mg/ml streptomycin at 37 °C.

2.6. Viability assay

Cell viability was tested by the 3-(4,5-dimethylthiazol-2-yl)-2,5-diphenyltetrazolium bromide (MTT) dye reduction assay modified as described before (Kotchetkov et al., 2005). Briefly, target cells were plated in triplicate (10,000 cells/well) in a 96-well white plate (Greiner Bio-One, Frickenhausen, Germany). The assay was optimized for the cell lines used in the experiments. The cells were incubated with different concentrations of nanoparticles: 0.01 mg/ml, 0.02 mg/ml, 0.06 mg/ml, 0.25 mg/ml, 0.5 mg/ml, 1.0 mg/ml, and 2.0 mg/ml. For the purposes of the experiments at the end of the incubation time (144 h), the solution was reacted for 2 h with 0.8 mg/ml of MTT (37 °C). Washing with PBS (1 ml) was followed by the addition of DMSO and 2.5 g SDS (1 ml), gentle shaking for 10 min so that complete dissolution was achieved. Aliquots (200 μl) of the resulting solutions were transferred in 96-well plates, and absorbance was recorded at 560 nm using the microplate spectrophotometer system (Spectra). Results were analysed with the SigmaPlot software (version 10.0) and are presented as percentage of the control values (unmodified HSA NPs and untreated cells, Fig. 3).

2.7. Cellular nanoparticle (NP) binding studies by flow cytometry

Cells were incubated with various concentrations of HSA NPs with adsorbed folic acid, HSA NPs with covalently bound folic acid, or unmodified HSA NPs for 4 h or 24 h. After 5 min, cells were trypsinised, harvested, washed twice with phosphate buffered saline (PBS), and analysed by flow cytometry using a FACSCalibur

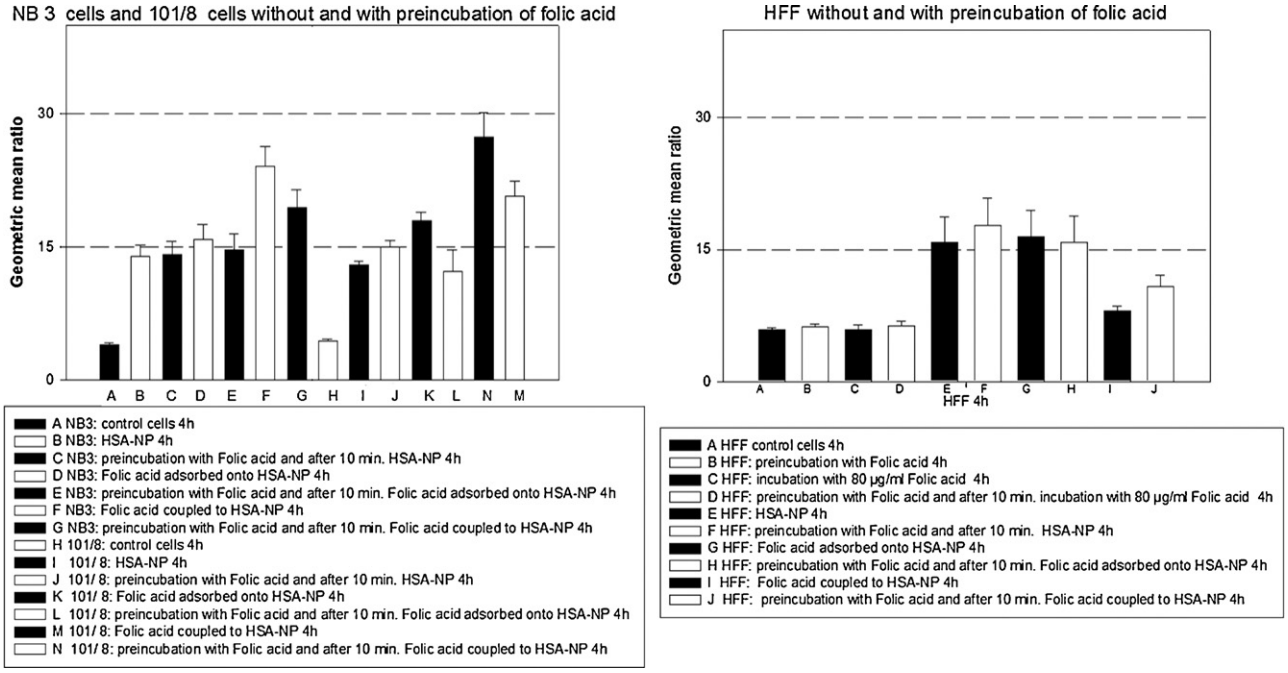

Fig. 4. Flow cytometric analysis of three cell lines: non-treated cells, with folic acid solution (800 μg) treated cells and binding of unmodified HSA NPs, HSA NPs with adsorbed folic acid, and HSA NPs with covalent folic acid to UKF-NB-3, 101/8, and HFF after 4 h with and without preincubation of 800 μg folic acid (mean ± S.D.; $n = 6$).

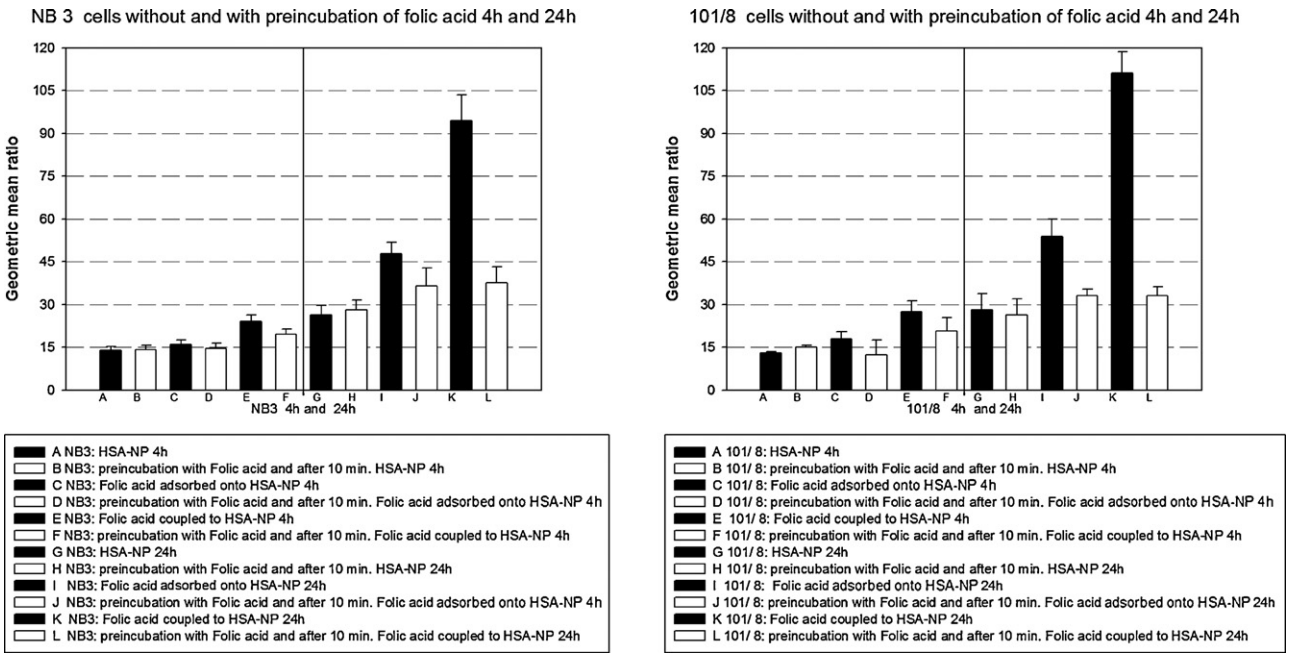

Fig. 5. Flow cytometric analysis of two cell lines: binding of unmodified HSA NPs, HSA NPs with adsorbed folic acid, and HSA NPs with covalent folic acid to UKF-NB-3 and 101/8 after 4 h and 24 h incubation with and without preincubation of 800 μg folic acid (mean ± S.D.; $n = 6$).

(BD, Heidelberg, Germany). HSA NPs show autofluorescence that can be detected at the FL-1 channel 530 nm. In order to investigate if folic acid specifically mediates cellular uptake, cells were pre-incubated with 800 μg/ml folic acid (a 10-fold excess concentration relative to NP-bound folic acid) for 10 min before adding HSA NPs with adsorbed folic acid, HSA NPs with covalently bound folic acid, or unmodified HSA NPs. Then, NP binding was analysed as described above.

2.8. Intracellular distribution and cellular uptake studies by confocal laser scanning microscopy (CLSM)

Cellular distribution experiments were performed with 101/8 cells and UKF-NB-3 cells. Cells were incubated with 80 μg/ml folic acid or 8 μg/mL folic acid bound to the surface of the HSA nanoparticles. Depending on the binding efficiency, NP concentrations between 8 and 12 mg/ml were used in cell culture medium at 37 °C for incubation times of 1, 4, 24, or 48 h. Then, cells were washed twice with PBS and stained for 2 min with 0.0005% (w/v) Alexa594-concanavalin A (staining the cell membrane) in PBS. After two further washing steps with PBS, cells were fixed with 500 μL ice-cold ethanol 70% (v/v) for 30 min. Ethanol was removed by washing three times with PBS. The slides were covered with Permount® medium (Fisher Science, Germany) and closed with cover glasses. The confocal microscopy study was performed with an Axiovert 200 M inverse microscope with a TCS SP% DIM6000 Meta device (Zeiss, Jena), argon ion laser ($\alpha = 488, 568, 647$ nm) and the LAS AF Image Examiner software. The green autofluorescence of the HSA

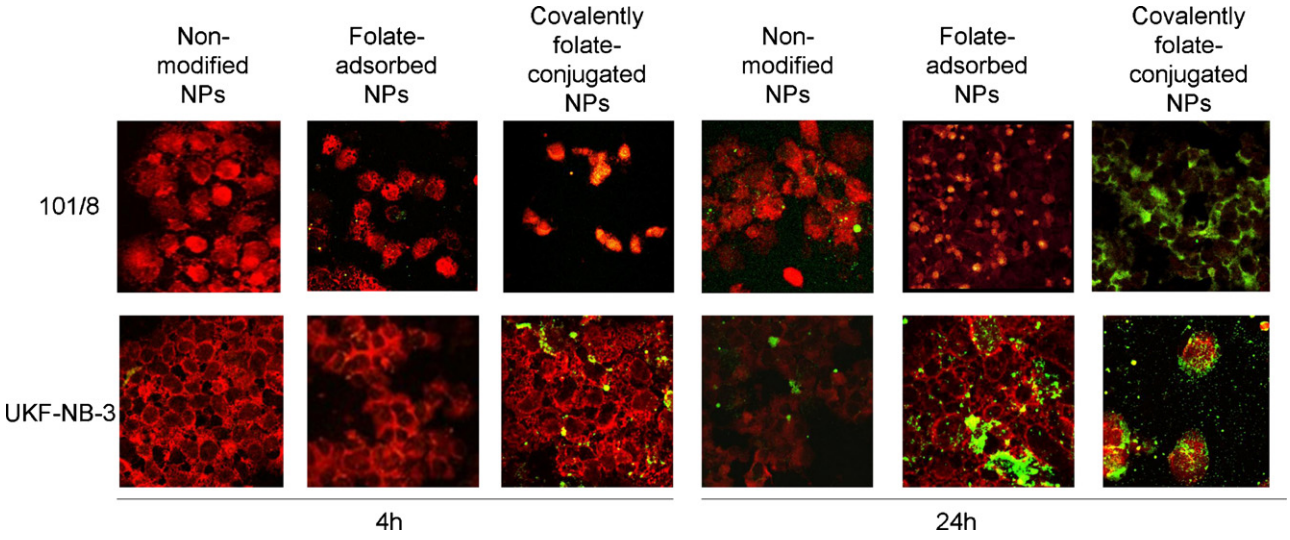

Fig. 6. Internalization and uptake of human serum albumin nanoparticles (HSA NPs) examined by laser confocal microscopy. The fluorescence intensities of the two cell lines 101/8 and UKF-NB-3 are shown after incubation of the cells with the following preparations: non-modified HSA NPs after 4 h (reference), folate-adsorbed HSA NPs, and covalently folate-conjugated HSA NPs. Two different incubation times were used: 4 h and 24 h. The fluorescence intensity and the cell images were obtained using two channels: green ($\lambda_{ex}/\lambda_{em}$ = 488/492–508 nm) for the autofluorescence of the HSA NPs and red ($\lambda_{ex}/\lambda_{em}$ = 568 nm/612–622 nm) for the conanavalin A Alexa594 incubated cell surface.

NPs was detected at 500 nm, the red fluorescence of Alexa594 at 617 nm.

2.9. Statistical analysis

BiAS for Microsoft Windows software, Version 9.05© 1989–2010 Epsilon was used for all statistical analyses. The data were subjected to the analysis of variance, and the means were compared using two-sided Student's *t*-test. Differences were considered to be significant at $P < 0.05$.

3. Results and discussion

The aim of the present study was to increase the uptake of HSA NPs into cancer cells through surface modification using folic acid. Different amounts of folic acid were attached to the NP surface by adsorption or by covalent coupling. Two tumour cell lines (UKF-NB-3, 101/8) and primary HFFs were used for this study.

3.1. Characterisation of nanoparticles

The unmodified nanoparticles had particle diameters of 156 ± 25 nm with a very narrow distribution (polydispersity index = 0.034 ± 0.022) as determined by photon correlation spectroscopy (PCS), indicating a monodisperse size distribution (Table 1). The coupling of the linker alone (EDC activated HSA NP) increased the diameter by 22 nm. NPs with adsorbed folate had a size of 280 ± 92 nm (polydispersity index = 0.030 ± 0.026). For the covalently folate-conjugated HSA NPs the average diameter was 239 ± 26 nm (polydispersity index = 0.030 ± 0.026). This is comparable to other previously used targeting moieties like transferrin and insulin (Ulbrich et al., 2009, 2011).

No statistically significant differences were observed between the zeta potentials of folate-conjugated NPs (-37 ± 8 mV), NPs with adsorbed folate (-40 ± 7 mV), NPs with linker but without folic acid (-30 ± 13 mV), or unmodified NPs (-42 ± 8 mV). Folate-linking, however, increased the particle density from 1.3270 ± 0.0407 g cm^{-3} to 1.5960 ± 0.0725 g cm^{-3} (two-sided Student's *t*-test $P < 0.05$ for comparison, $n = 3$) which may influence particle uptake (Alberola and Radler, 2009). The HSA nanoparticles were of spherical shape (Fig. 1).

A slight increase in particle size and polydispersity occurred in the cell culture medium (Table 2). Therefore, NPs were sonicated prior to addition to cells in order to prevent agglomeration.

3.2. Determination of folic acid content

The binding efficacy was calculated as the difference between the total amount of folic acid and the amount of non-bound folic acid determined after centrifugation of NPs in the supernatant during the first washing step (Fig. 2). About 169 mol folic acid/g HSA were linked to the HSA NPs. After conjugation, the number of folic acid molecules bound to the NP surface approximately corresponded to the decrease of the number of surface amino groups of HSA NPs indicating that folic acid was coupled to the HSA amino groups. The percentage of binding to the surface of the nanoparticles amounted to 95.8 ± 0.4% of the added folic acid in the case of its covalent attachment and 98.5 ± 1.5% after its adsorption (Table 1 and Fig. 2).

The number of amino groups on HSA NPs surfaces decreased from 499 ± 17 mol/g HSA on non-conjugated NPs to 340 ± 23 mol/g HSA on folate-conjugated HSA NPs, as determined by Flouraldehyde™ amino assay (two-sided Student's *t*-test $P < 0.05$ for comparison, $n = 3$).

3.3. Cell viability

Among the components of the NPs, only N-(3-dimethylaminopropyl)-N-ethylcarbodiimide (EDC) was expected to exhibit cytotoxicity, because cationic polymers may strongly interact with anionic cellular surfaces and therefore compromise the integrity of cellular membranes (Wei et al., 2009). HSA NPs prepared with EDC and folic acid had no influence on cell viability in HFF cells but decreased the viability of UKF-NB-3 cells (IC50 = 0.24 mg/ml) and 101/8 cells (IC50 = 0.54 mg/ml) at high concentrations, as indicated by MTT assay (Fig. 3). HSA NP concentrations used for cell binding- and uptake-studies did not affect cell viability.

3.4. Cellular binding and uptake of HSA NPs

UKF-NB-3 cells, 101/8 cells, and HFFs showed similar cell binding of non-modified HSA NPs. Folic acid (800 μg/ml) did not influence cell binding of non-modified HSA NPs (Fig. 4). Covalent linkage of folic acid increased HSA NP binding to UKF-NB-3 and 101/8 cells but decreased HSA NP binding to HFFs (Figs. 4 and 5). Folic acid adsorption to HSA NPs increased HSA NP binding to cancer cells to a much lesser extent compared to folate-conjugated HSA NPs. Differential behaviour of folate-conjugated HSA NP in cancer cells and normal cells may be explained by increased FR expression levels in cancer cells and/or preferential expression of α-FRs (specific for free R-carboxylic acid of the folic acid on the HSA NP surface) in cancer cells and preferential expression of β-FRs (higher affinity the reduced form of folic acid, 5-methyltetrahydrofolate) on normal cells (Sudimack and Lee, 2000; Elnakat and Ratnam, 2004; Park et al., 2005; Parker et al., 2005; Leamon, 2008; Markert et al., 2008).

Pre-incubation with folic acid decreased binding of covalently folate-conjugated HSA NPs and folate-adsorbed HSA NPs to UKF-NB-3 and 101/8 cells to the level of non-modified HSA-NPs (Figs. 4 and 5) suggesting that the increased uptake is specifically mediated through interaction of conjugated folate with the folate receptor.

CLSM pictures showed that covalent linkage of folate not only increased HSA NP binding to the cell surface but also increased HSA NP uptake (Fig. 6). The fluorescence intensity of cells incubated with covalently folate-conjugated HSA NPs was significantly higher, especially after 24 h, than that of cells incubated with folic acid adsorbed onto the surface of HSA NPs. The fluorescence intensity in cells exposed to NPs (folate-adsorbed HSA NPs, covalently folate-conjugated HSA NPs, unmodified HSA NPs) increased with incubation time (Fig. 6). Similar results had been obtained by flow cytometric analysis (Figs. 4 and 5). NPs without folic acid yielded a weaker fluorescence (Fig. 6) compared to folate-conjugated HSA NPs and folate-adsorbed HSA NPs with the tumour cells (Fig. 6). In summary, these flow cytometry and CLSM data demonstrate the specific targeting and intracellular uptake of folic acid modified HSA NPs.

4. Conclusion

Covalently folate-conjugated HSA NPs show increased binding to and uptake into the investigated cancer cell lines UKF-NB-3 and 101/8 compared to non-modified or folate-adsorbed HSA NPs. In contrast, folate binding did not increase HSA-NP binding to or uptake into normal HFFs. Our data suggest that covalently folate-conjugated HSA NPs represent a drug delivery system that shows specifity for cancer cells.

Acknowledgments

We are thankful to Martina Scholz for the HFF cell preparation. This work was supported by the Hilfe für krebskranke Kinder Frankfurt e.V. und der Frankfurter Stiftung für krebskranke Kinder.

References

Alberola, A.P., Radler, J.O., 2009. The defined presentation of nanoparticles to cells and their surface controlled uptake. Biomaterials 30, 3766–3770.

Bae, Y., Jang, W.D., Nishiyama, N., Fukushima, S., Kataoka, K., 2005. Multifunctional polymeric micelles with folate-mediated cancer cell targeting and pH-triggered drug releasing properties for active intracellular drug delivery. Mol. Biosyst. 1, 242–250.

Barratt, G., 2003. Colloidal drug carriers: achievements and perspectives. Cell Mol. Life Sci. 60, 21–37.

Cinatl Jr., J., Cinatl, J, Rabenau, H., Gumbel, H.O., Kornhuber, B., Doerr, H.W., 1994. In vitro inhibition of human cytomegalovirus replication by desferrioxamine. Antivir. Res. 25, 73–77.

Ciofani, G., Raffa, V., Menciassi, A., Cuschieri, A., 2008. Folate functionalized boron nitride nanotubes and their selective uptake by glioblastoma multiforme cells: Implications for their use as boron carriers in clinical boron neutron capture therapy. Nanoscale Res. Lett. 4, 113–121.

Dosio, F., Arpicco, S., Stella, B., Brusa, P., Cattel, L., 2009. Folate-mediated targeting of albumin conjugates of paclitaxel obtained through a heterogeneous phase system. Int. J. Pharm. 382, 117–123.

Elnakat, H., Ratnam, M., 2004. Distribution, functionality and gene regulation of folate receptor isoforms: implications in targeted therapy. Adv. Drug Deliv. Rev. 56, 1067–1084.

Esmaeili, F., Ghahremani, M.H., Ostad, S.N., Atyabi, F., Seyedabadi, M., Malekshahi, M.R., Amini, M., Dinarvand, R., 2008. Folate-receptor-targeted delivery of docetaxel nanoparticles prepared by PLGA-PEG-folate conjugate. J. Drug Target. 16, 415–423.

Feng, C., Wang, T., Tang, R., Wang, J., Long, H., Gao, X., Tang, S., 2010. Silencing of the MYCN gene by siRNA delivered by folate receptor-targeted liposomes in LA-N-5 cells. Pediatr. Surg. Int. 26, 1185–1191.

Gao, J., Chen, K., Xie, R., Xie, J., Lee, S., Cheng, Z., Peng, X., Chen, X., 2009. Ultrasmall near-infrared non-cadmium quantum dots for in vivo tumor imaging. Small 6, 256–261.

Hattori, Y., Shi, L., Ding, W., Koga, K., Kawano, K., Hakoshima, M., Maitani, Y., 2009. Novel irinotecan-loaded liposome using phytic acid with high therapeutic efficacy for colon tumors. J. Controlled Release 136, 30–37.

Heister, E., Lamprecht, C., Neves, V., Tîlmaciu, C., Datas, L., Flahaut, E., Soula, B., Hinterdorfer, P., Coley, H.M., Silva, S.R., McFadden, J., 2009. Higher dispersion efficacy of functionalized carbon nanotubes in chemical and biological environments. ACS Nano 4, 2615–2626.

Hekmatara, T., Bernreuther, C., Khalansky, A.S., Theisen, A., Weissenberger, J., Gelperina, S., Kreuter, J., Glatzel, M., 2009. Efficient systemic therapy of rat glioblastoma by nanoparticle-bound doxorubicin is due to antiangiogenic effects. Clin. Neuropathol. 28, 153–164.

Kotchetkov, R., Driever, P.H., Cinatl, J., Michaelis, M., Karaskova, J., Blaheta, R., Squire, J.A., Von Deimling, A., Moog, J., Cinatl Jr., J., 2005. Increased malignant behavior in neuroblastoma cells with acquired multi-drug resistance does not depend on P-gp expression. Int. J. Oncol. 27, 1029–1037.

Kukowska-Latallo, J.F., Candido, K.A., Cao, Z., Nigavekar, S.S., Majoros, I.J., Thomas, T.P., Balogh, L.P., Khan, M.K., Baker Jr., J.R., 2005. Nanoparticle targeting of anticancer drug improves therapeutic response in animal model of human epithelial cancer. Cancer Res. 65, 5317–5324.

Langer, K., Coester, C., Weber, C., von Briesen, H., Kreuter, J., 2000. Preparation of avidin-labeled protein nanoparticles as carriers for biotinylated peptide nucleic acid. Eur. J. Pharm. Biopharm. 49, 303–307.

Leamon, C.P., 2008. Folate-targeted drug strategies for the treatment of cancer. Curr. Opin. Investig. Drugs 9, 1277–1286.

Li, Y., Qi, X.R., Maitani, Y., Nagai, T., 2009. PEG-PLA diblock copolymer micelle-like nanoparticles as all-trans-retinoic acid carrier: in vitro and in vivo characterizations. Nanotechnology 20, 55106.

Ma, P.X., 2008. Biomimetic materials for tissue engineering. Adv. Drug Deliv. Rev. 60, 184–198.

Maeda, H, Wu, J., Sawa, T., Matsumura, Y., Hori, K., 2000. Tumor vascular permeability and the EPR effect in macromolecular therapeutics: a review. J. Controlled Release 65, 271–284.

Maris, J.M., Hogarty, M.D., Bagatell, R., Cohn, S.L., 2007. Neuroblastoma. Lancet 369, 2106–2120.

Markert, S., Lassmann, S., Gabriel, B., Klar, M., Werner, M., Gitsch, G., Kratz, F., Hasenburg, A., 2008. Alpha-folate receptor expression in epithelial ovarian carcinoma and non-neoplastic ovarian tissue. Anticancer Res. 28, 3567–3572.

Michaelis, M., Langer, K., Arnold, S.C., Hinsch, N., Rothweiler, F., Deubzer, H.E., Witt, O., Langer, K., Doerr, H.W., Wels, W.S., Cinatl Jr., J., 2004. Pharmacological activity of DTPA linked to protein-based drug carrier systems. Biochem. Biophys. Res. Commun. 323, 1236–1240.

Nie, Y., Zhang, Z., Li, L., Luo, K., Ding, H., Gu, Z., 2009. Synthesis, characterization and transfection of a novel folate-targeted multipolymeric nanoparticles for gene delivery. J. Mater. Sci.-Mater. Med. 20, 1849–1857.

Park, E.K., Lee, S.B., Lee, Y.M., 2005. Preparation and characterization of methoxy poly(ethylene glycol)/poly(epsilon-caprolactone) amphiphilic block copolymeric nanospheres for tumor-specific folate-mediated targeting of anticancer drugs. Biomaterials 26, 1053–1061.

Parker, N., Turk, M.J., Westrick, E., Lewis, J.D., Low, P.S., Leamon, C.P., 2005. Folate receptor expression in carcinomas and normal tissues determined by a quantitative radioligand binding assay. Anal. Biochem. 338, 284–293.

Prabaharan, M., Grailer, J.J., Pilla, S., Steeber, D.A., Gong, S., 2009. Folate-conjugated amphiphilic hyperbranched block copolymers based on Boltorn H40, poly(L-lactide) and poly(ethylene glycol) for tumor-targeted drug delivery. Biomaterials 30, 3009–3019.

Steinhauser, I., Spankuch, B., Strebhardt, K., Langer, K., 2006. Trastuzumab-modified nanoparticles: optimisation of preparation and uptake in cancer cells. Biomaterials 27, 4975–4983.

Steiniger, S.C., Kreuter, J., Khalansky, A.S., Skidan, I.N., Bobruskin, A.I., Smirnova, Z.S., Severin, S.E., Uhl, R., Kock, M., Geiger, K.D., Gelperina, S.E., 2004. Chemotherapy of glioblastoma in rats using doxorubicin-loaded nanoparticles. Int. J. Cancer 109, 759–767.

Sudimack, J., Lee, R.J., 2000. Targeted drug delivery via the folate receptor. Adv. Drug Deliv. Rev. 41, 147–162.

Thomas, T.P., Shukla, R., Kotlyar, A., Kukowska-Latallo, J., Baker Jr., J.R., 2010. Dendrimer-based tumor cell targeting of fibroblast growth factor-1. Bioorg. Med. Chem. Lett. 20, 700–703.

Tosi, G., Costantino, L., Ruozi, B., Forni, F., Vandelli, M.A., 2008. Polymeric nanoparticles for the drug delivery to the central nervous system. Expert Opin. Drug Deliv. 5, 155–174.

Ulbrich, K., Hekmatara, T., Herbert, E., Kreuter, J., 2009. Transferrin- and transferrin-receptor-antibody-modified nanoparticles enable drug delivery across the blood–brain barrier (BBB). Eur. J. Pharm. Biopharm. 71, 251–256.

Ulbrich, K., Knobloch, T., Kreuter, J., 2011. Targeting the insulin receptor: nanoparticles for drug delivery across the blood–brain barrier (BBB). J. Drug Target. 19, 125–132.

Vandervoort, J., Ludwig, A., 2002. Biocompatible stabilizers in the preparation of PLGA nanoparticles: a factorial design study. Int. J. Pharm. 238, 77–92.

Wartlick, H., Michaelis, K., Balthasar, S., Strebhardt, K., Kreuter, J., Langer, K., 2004. Highly specific HER2-mediated cellular uptake of antibody-modified nanoparticles in tumour cells. J. Drug Target. 12, 461–471.

Weber, C., Kreuter, J., Langer, K., 2000. Desolvation process and surface characteristics of HSA-nanoparticles. Int. J. Pharm. 196, 197–200.

Wei, Y., Jana, N.R., Tan, S.J., Ying, J.Y., 2009. Surface coating directed cellular delivery of TAT-functionalized quantum dots. Bioconjug. Chem. 20, 1752–1758.

Wen, P.Y., Kesari, S., 2008. Malignant gliomas in adults. New Engl. J. Med. 359, 492–507.